J. Math. Anal. Appl. 451 (2017) 1165–1178

Contents lists available at ScienceDirect

Journal of Mathematical Analysis and Applications

www.elsevier.com/locate/jmaa

Bistability in a model of grassland and forest transition

Deqiong Ding [a,b], Junping Shi [b,*], Yan Wang [b,c]

[a] Department of Mathematics, Harbin Institute of Technology at Weihai, Weihai, Shandong, 264209, PR China
[b] Department of Mathematics, College of William and Mary, Williamsburg, VA, 23187-8795, USA
[c] Department of Applied Science, College of William and Mary, Williamsburg, VA, 23187-8795, USA

ARTICLE INFO

Article history:
Received 25 September 2016
Available online 4 March 2017
Submitted by Y. Du

Keywords:
Grassland and forest transition model
Nonlinear response function
Multiple equilibria
Bistability
Bifurcation

ABSTRACT

It is acknowledged that the role of fire and climate in determining savanna and forest distributions requires comprehensive theoretical reevaluation. In this paper, an ordinary differential equation model describing the grassland and forest transition is considered. We use a modified Hill function as the nonlinear response of fire frequency to grass abundance, and the global dynamics of the model is completely classified. It is shown that any solution converges to an equilibrium, and the system has one, two or three coexistence equilibria depending on parameter values. Our results provide precise parameter range of bistability.

1. Introduction

Vegetation growth responding to climate changes is one of the core topics regarding global environment change. There is growing evidence within the environmental science community that our planet has entered a potentially catastrophic phase of human-induced global climate warming [9,10]. Human activity has a huge impact on the changing of vegetation. Excessive deforestation, tourism development, urban expansion all influence the amount of tree cover and destroy huge area of forest.

The tree cover is influenced by complex interaction between climate, human activity, animals, soil and many other unexpected disturbances. It is interesting that in some area where the environmental conditions suggest that forest should dominant, it turns out to be savanna prevailing [19]. Also an intermediate level of tree cover rarely happens, and there is a transition from the savanna state to the forest state when the environmental condition changes. This suggests that in the ecosystem, there are two alternative stable states corresponding to savanna (low tree cover), forest (high tree cover) respectively, and an unstable state

* Corresponding author.
E-mail address: jxshix@wm.edu (J. Shi).

http://dx.doi.org/10.1016/j.jmaa.2017.02.062
0022-247X/

(intermediate tree cover). The main factors driving force in determining the distribution of tree cover are the rainfall and fires, and the bistability here is due the positive feedback of fire interaction [15,16].

According to the data collected form satellite in [16], when the mean annual rainfall is less than 1000 mm, fire is less important since water becomes the main factor of limiting the tree growth. In this situation, tree cover often maintains at a relatively low level which may be savanna state. When the mean annual rainfall is more than 2000 mm, fire will be less likely to happen because such heavy rain leads to forest state. Only when the mean annual rainfall is between 1000 mm and 2000 mm, fire plays a key role in differentiating low and high tree cover. It was shown in [19] that fire can restrict the tree cover while climate and other external environmental conditions hold lush forest. As long as fire can reduce tree cover, the grass biomass drops off rapidly as tree cover increases [13]. Thus fire mainly spread on the land with tree cover less than 40% [1]. Also fire does not destroy the saplings which will sprout after. So fire drives the tree recruitment as a positive feedback [12,20].

In [16] the authors proposed a system of three ordinary differential equations of grass, tree saplings, and adult trees which incorporates the fire feedback with a nonlinear response function depending on grass abundance. So in their model the tree cover is determined by the combined interaction of rainfall and fire. While some qualitative analysis was conducted in [16] in a formal way, here we use a more specific nonlinear response function to quantify the model. Moreover we rigorously show the existence of precisely three positive steady states, and we also obtain exact parameter ranges of bistable dynamics. We also show that there are no limit cycles in the system, hence oscillatory states cannot occur. Note that in another system of four equations of grass, savanna saplings, savanna trees and forest trees [17], time-periodic states were found for certain parameter values. The spatial effect to the model was also considered in [12].

Bistability and corresponding hysteresis phenomena have arisen in various ecological systems via different mechanisms [2,4]. A classical example is the spruce budworm outbreak [7], and a general description is provided in [9]. More recently bistability (or alternative stable states) has also been found in shallow lake dynamics [11], eutrophication of aquatic ecosystems [3], coral reef dynamics [6,8], and oyster population dynamics [5].

In Section 2 we describe the differential equation model in details, and in Section 3 we present our main mathematical results accompanied by numerical simulations. Some concluding remarks are given in Section 4.

2. Model

We consider an ordinary differential equation model proposed by [16]:

$$\begin{cases} G' = \mu S + \gamma T - \beta G T, \\ S' = \beta G T - \omega(G) S - \mu S, \\ T' = \omega(G) S - \gamma T. \end{cases} \tag{2.1}$$

Here G is the total area of grass, S is the total area of tree saplings and T is the total area of adult trees. In (2.1), μ and γ are the mortality rates of saplings and trees respectively. After their death, the areas of saplings and trees revert to the one for grass in proportion to the number of trees and saplings. Hence the grassland recruitment is in form of $\mu S + \gamma T$. On the other hand the grassland loses its area when the adult trees establish saplings on. It is assumed that the saplings can only be successfully established on the grassland proportional to adult trees with a rate β. The growth rate of trees is proportional to the number of saplings with a nonlinear requirement rate $\omega(G)$ depending on the grassland. Indeed a higher value of G induces a higher possibility of fire, that implies a lower tree recruitment $\omega(G)$; while a lower value of G reduces the probability of fire and it increases the tree recruitment. Hence the fire feedback process is modeled by the nonlinear function $\omega(G)$. In [16], it is proposed that $\omega(G)$ is a sigmoidal function of grass

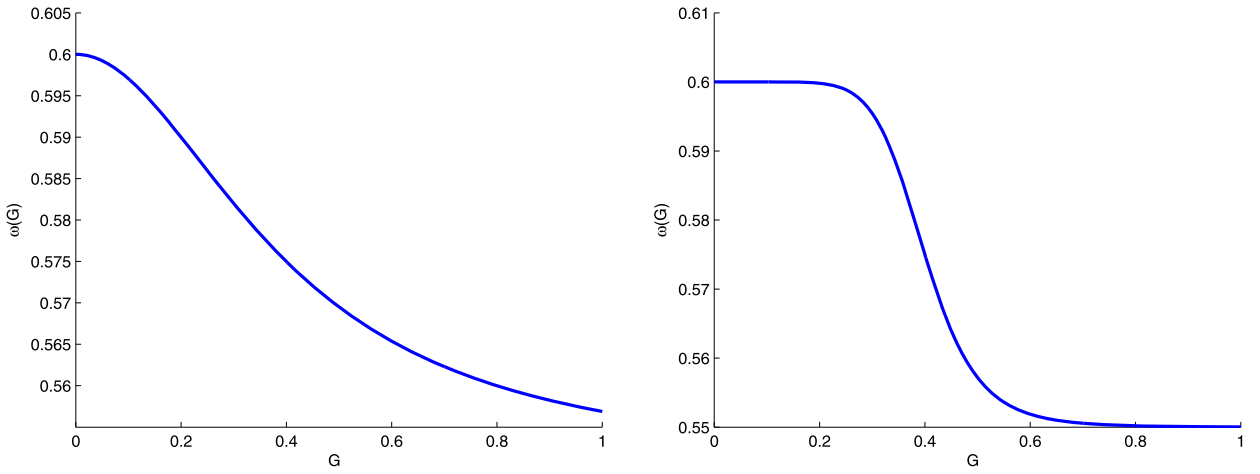

Fig. 1. Graph of sigmoid recruitment function $\omega(G)$ defined in (2.2). Here $M = 0.6$, $m = 0.55$, $h = 0.4$, and $n = 2$ (left), $n = 8$ (right).

cover, and the functional form is determined by the forest-savanna dynamics. But they did not give a specific expression of the fire factor in their model.

In order to obtain more detailed theoretical results, we propose the tree recruitment rate $\omega(G)$ (see Fig. 1) to be

$$\omega(G) = \frac{Mh^n + mG^n}{h^n + G^n}, \tag{2.2}$$

where $m,\ M,\ h > 0$ satisfying $M > m$, and $n > 1$. It is easy to verify that the tree recruitment function $\omega(G)$ satisfies following properties:

1. $m \le \omega(G) \le M$ for $G \ge 0$;
2. $\omega(0) = M$, $\omega'(0) = 0$, $\omega'(G) < 0$ for $G \ge 0$, and $\lim\limits_{G\to\infty} \omega(G) = m$;
3. $\omega(h) = \dfrac{M+m}{2}$ and $\omega''(h) = 0$, so $G = h$ is the half-saturation point where the graph of $\omega(G)$ changes from concave down to concave up.

Therefore the maximum tree recruitment rate M is achieved when there is no grassland, and the minimum tree recruitment rate m occurs when there is a large amount of grassland. The upper bound M and the lower bound m of the function $\omega(G)$ are affected by the annual rainfall. The half-saturation point h can often be interpreted as the transition point from the high recruitment rate to the low one. According to the empirical analysis in [16], fire spreads only at tree cover of 40% or less.

The parameter n affects the shape of the sigmoid function, and when n is large, the function $\omega(G)$ is more similar to a Heaviside type switch function switching from M to m at $G = h$ (see Fig. 1). This is a character of Hill's function or Holling type III functional response, which is used widely in biological models [3,7].

Since in Eq. (2.1), $(G + S + T)' = 0$ thus $G + S + T = C_0$ for some $C_0 > 1$. Without loss of generality, we assume $C_0 = 1$ otherwise we can consider the quantities G/C_0, S/C_0 and T/C_0 instead. Then Eq. (2.1) is equivalent to

$$\begin{cases} G' = \mu(1 - G - T) + \gamma T - \beta GT, \\ T' = \omega(G)(1 - G - T) - \gamma T. \end{cases} \tag{2.3}$$

In the following we take $\omega(G)$ to be the one defined in (2.2) with $n = 2$, then (2.3) becomes

$$\begin{cases} G' = \mu(1 - G - T) + \gamma T - \beta GT, \\ T' = \left(\dfrac{Mh^2}{h^2 + G^2} + \dfrac{mG^2}{h^2 + G^2}\right)(1 - G - T) - \gamma T, \\ G(0) = G_0,\ T(0) = T_0. \end{cases} \tag{2.4}$$

In the following we mainly consider the dynamical behavior of system (2.4).

3. Analysis

3.1. Boundedness and nonexistence of limit cycles

Firstly we derive some basic properties of solutions of system (2.4), such as the boundedness and nonexistence of limit cycles. According to the biological setting of the model described above, we define

$$\Omega = \{(G, T) : G > 0, T > 0, G + T < 1\}. \tag{3.1}$$

Then we have

Theorem 3.1. *Let Ω be defined as in Eq. (3.1), and let $\bar{\Omega}$ be the closure of Ω including the boundary $\partial\Omega$.*

(1) Suppose that $(G_0, T_0) \in \bar{\Omega}$, then Eq. (2.4) has a unique solution $(G(t), T(t))$ for $t \in (0, \infty)$, and $(G(t), T(t)) \in \bar{\Omega}$ for all $t > 0$ so Ω is positively invariant for Eq. (2.4).
(2) System (2.4) has no periodic orbits in Ω.

Proof. The vector field defined by system (2.4) is smooth in Ω, which guarantees the local existence and uniqueness of solutions of system (2.4). We show that the orbits starting from $\bar{\Omega}$ cannot escape $\bar{\Omega}$ from the boundary $\partial\Omega = \partial\Omega_1 \bigcup \partial\Omega_2 \bigcup \partial\Omega_3$, where $\partial\Omega_1 = \{(G, T) : 0 \le G \le 1, T = 0\}$, $\partial\Omega_2 = \{(G, T) : 0 \le T \le 1, G = 0\}$ and $\partial\Omega_3 = \{(G, T) : G > 0, T > 0, G + T = 1\}$, so the existence of solution is global. If $(G_0,\ T_0) \in \partial\Omega_1$, then $T_0 = 0$, $T' = \omega(G)(1 - G) > 0$ for $0 \ge G < 1$. If $(G_0,\ T_0) \in \partial\Omega_2$, then $G_0 = 0$, $G' = \mu(1 - T) + \gamma T > 0$, for $0 \ge T \ge 1$. If $(G_0,\ T_0) \in \partial\Omega_3$, we define $X = G + T$. Then, on the upper boundary $\partial\Omega_3$, we have

$$\frac{dX}{dt} = \frac{dG}{dt} + \frac{dT}{dt} = -\beta GT < 0.$$

That is, if $(G_0,\ T_0) \in \bar{\Omega}$ then $(G(t),\ T(t)) \in \bar{\Omega}$ for all $t > 0$. Hence all orbits starting from $\bar{\Omega}$ stay in $\bar{\Omega}$ for all time $t > 0$.

To exclude the possibility of periodic orbit, we apply the classical Bendixion criterion. Denote

$$\begin{cases} G' = \mu(1 - G - T) + \gamma T - \beta GT \triangleq P(G, T), \\ T' = \dfrac{Mh^2 + mG^2}{h^2 + G^2}(1 - G - T) - \gamma T \triangleq Q(G, T). \end{cases} \tag{3.2}$$

An easy computation yields that

$$\frac{\partial P}{\partial G} + \frac{\partial Q}{\partial T} = -\mu - \beta T - \frac{Mh^2 + mG^2}{G^2 + h^2} - \gamma < 0.$$

Therefore the Bendixion criterion [18] can be applied to system (2.4) in Ω and there exist no periodic orbits in Ω. □

3.2. Existence and multiplicity of equilibria

In this subsection, we show the existence and multiplicity of the equilibria. Based on biological meaning, we ask all equilibria to be nonnegative. An equilibrium satisfies the following equations:

$$\begin{cases} \mu(1-G-T)+\gamma T-\beta GT=0, \\ w(G)(1-G-T)-\gamma T=0. \end{cases} \tag{3.3}$$

Hence it is straightforward to calculate that system (2.4) has only one boundary equilibrium $E^0=(1,0)$.

Next we consider the coexistence equilibrium $E^*=(G^*,T^*)$ such that $G^*,T^*\in(0,1)$ and $G^*+T^*\leq 1$. By using the first equation of system (3.3), we get

$$T=\frac{\mu(1-G)}{\mu+\beta G-\gamma}. \tag{3.4}$$

Substituting into the second equation of system (3.3), we obtain

$$w(G)=\frac{\mu\gamma}{\beta G-\gamma}\triangleq f(G). \tag{3.5}$$

Since $w(G)\geq 0$, then there exists a coexistence equilibrium if and only if $\beta G-\gamma>0$. Furthermore, because of $0\leq G\leq 1$, then system (2.4) does not have coexistence equilibria if $\beta\leq\gamma$. Indeed if $\beta\leq\gamma$, it is easy to show that all positive solutions converge to $E^0=(1,0)$ from Theorem 3.1. Also if G satisfies (3.5), $\beta G-\gamma>0$ hence $T>0$. Therefore in the following we always assume that $\beta>\gamma>0$.

Set

$$F(G)=w(G)-f(G),\quad \text{and}\quad p(G)=\frac{(G^2+h^2)(\beta G-\gamma)}{m\beta}F(G). \tag{3.6}$$

From Eq. (3.4), any positive root of $F(G)=0$ or $p(G)=0$ satisfying $G<1$ corresponds to a coexistence equilibrium of system (2.4). From simple calculation, we have

$$\begin{aligned} p(G)&=G^3-\frac{(\mu+m)\gamma}{m\beta}G^2+\frac{Mh^2}{m}G-\frac{(\mu+M)h^2\gamma}{m\beta} \\ &\triangleq G^3+p_1G^2+p_2G+p_3, \end{aligned} \tag{3.7}$$

where

$$p_1=-\frac{(\mu+m)\gamma}{m\beta},\quad p_2=\frac{Mh^2}{m},\quad p_3=-\frac{(\mu+M)h^2\gamma}{m\beta}. \tag{3.8}$$

Since $p_3<0$, then $p(0)<0$ and $p(G)\to\infty$ as $G\to\infty$, thus $p(G)=0$ has at least one positive root. Differentiating $p(G)$, we get

$$p'(G)=3G^2+2p_1G+p_2. \tag{3.9}$$

If $p_1^2\leq 3p_2$, then $p'(G)\geq 0$ and $p(G)$ is nondecreasing. It is easily seen that $p(G)$ has a unique simple positive root (see Fig. 2 (f)). If $p_1^2>3p_2$, then $p'(x)=0$ has two zeros:

$$x_1=-\frac{p_1}{3}-\frac{1}{3}\sqrt{p_1^2-3p_2},\quad x_2=-\frac{p_1}{3}+\frac{1}{3}\sqrt{p_1^2-3p_2}. \tag{3.10}$$

Table 1
Parameters values for simulations of equation (2.4).

Parameter	μ	γ	M	m	h
Value	0.3	0.025	0.6	0.012	0.063

Since $p_1 < 0$ and $p_2 > 0$, then we have $0 < x_1 < x_2$. Furthermore, since $p_3 < 0$, according to the Appendix C in [14], we have that if $p(x_1)p(x_2) > 0$, then $p(x)$ has a unique positive zero (see Fig. 2 (a) and (e)); if $p(x_1)p(x_2) = 0$, then $p(x)$ has two positive zeros (see Fig. 2 (b) and (d)); and if $p(x_1)p(x_2) < 0$, then there are three positive zeros (such as Fig. 2 (c)). Fig. 2 shows the evolution of the graphs of $p(G)$ when varying β, while the values of other parameters are given by the ones in Table 1.

By straightforward calculation, we get

$$\begin{aligned} p(x_1)p(x_2) &= \frac{1}{27}(-p_1^2p_2^2 + 4p_2^3 + 4p_1^3p_3 + 27p_3^2 - 18p_1p_2p_3) \\ &\triangleq \frac{1}{27\beta^4}(A\beta^4 + B\beta^2 + C) \triangleq \frac{1}{27\beta^4}\Delta(\beta^2), \end{aligned} \tag{3.11}$$

where $\Delta(x) = Ax^2 + Bx + C$ is a quadratic polynomial with

$$\begin{aligned} A &= \frac{4M^3h^6}{m^3}, \quad C = \frac{4(\mu+m)^3(\mu+M)\gamma^4h^2}{m^4}, \\ B &= \frac{h^4}{m^2}\left[-\left(\frac{(\mu+m)\gamma M}{m}\right)^2 + 27(\mu+M)^2\gamma^2 - \frac{18(\mu+m)(\mu+M)\gamma^2M}{m}\right]. \end{aligned} \tag{3.12}$$

To shorten our notations, we introduce a new parameter

$$a = \frac{M(m+\mu)}{m(M+\mu)}. \tag{3.13}$$

Clearly $a > 1$ since $M > m$ and we can calculate that

$$B = -\frac{h^4\gamma^2(\mu+M)^2}{m^2}(a^2 + 18a - 27), \quad B^2 - 4AC = \frac{h^8\gamma^4(\mu+M)^4}{m^4}(a-1)(a-9)^3. \tag{3.14}$$

From the solutions of quadratic equation $\Delta(x) = 0$, we obtain that

(1) If $a > 9$, then $B < 0$ and $B^2 - 4AC \geq 0$. That is, $\Delta(x)$ has two zeros H_1^2 and H_2^2 defined by

$$\begin{aligned} H_1 &= \frac{\gamma(\mu+m)}{mha}\sqrt{\frac{m+\mu-ma}{\mu a}}\left\{(a^2+18a-27) - \sqrt{(a-1)(a-9)^3}\right\}^{1/2}, \\ H_2 &= \frac{\gamma(\mu+m)}{mha}\sqrt{\frac{m+\mu-ma}{\mu a}}\left\{(a^2+18a-27) + \sqrt{(a-1)(a-9)^3}\right\}^{1/2}. \end{aligned} \tag{3.15}$$

Clearly $H_2 > H_1 > 0$. Since $\beta > 0$ and $A > 0$, then we obtain that

(i) If $0 < \beta < H_1$ or $H_2 < \beta \leq \dfrac{(\mu+m)\gamma}{h\sqrt{mM}}$, then $p(x_1)p(x_2) > 0$;

(ii) If $\beta = H_1$ or $\beta = H_2$, then $p(x_1)p(x_2) = 0$;

(iii) If $H_1 < \beta < H_2$, then $p(x_1)p(x_2) < 0$.

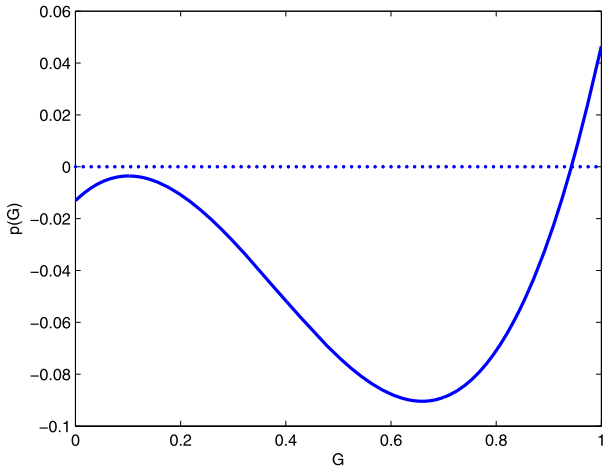

(a) $\beta = 0.57$

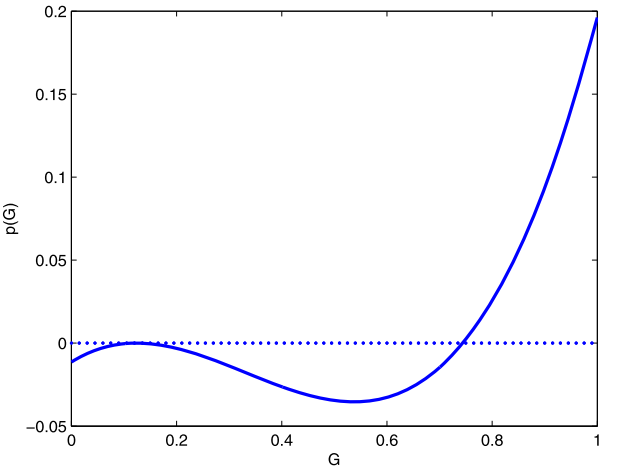

(b) $\beta = 0.6551$

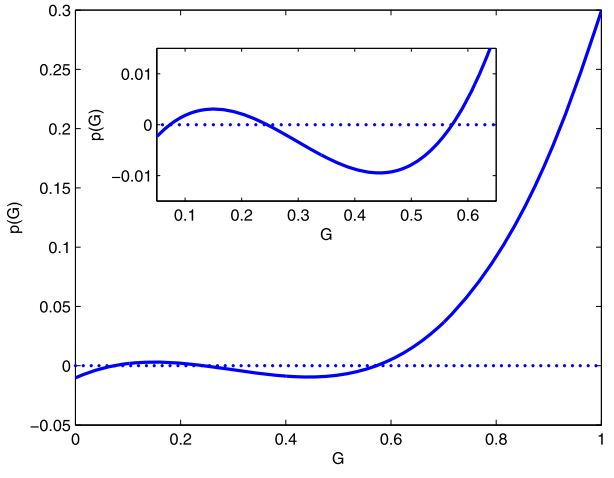

(c) $\beta = 0.73$

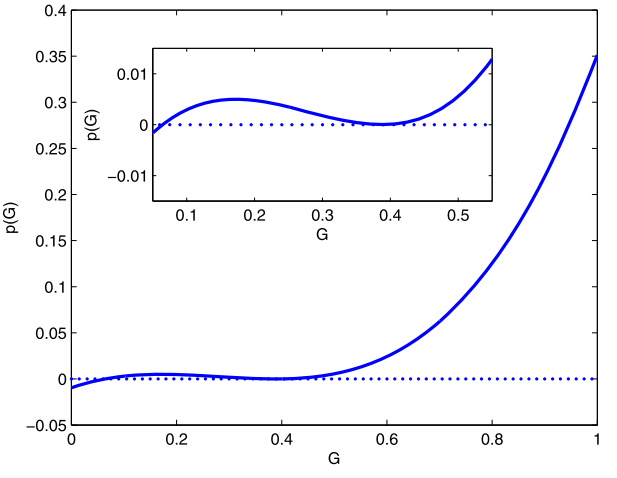

(d) $\beta = 0.7746$

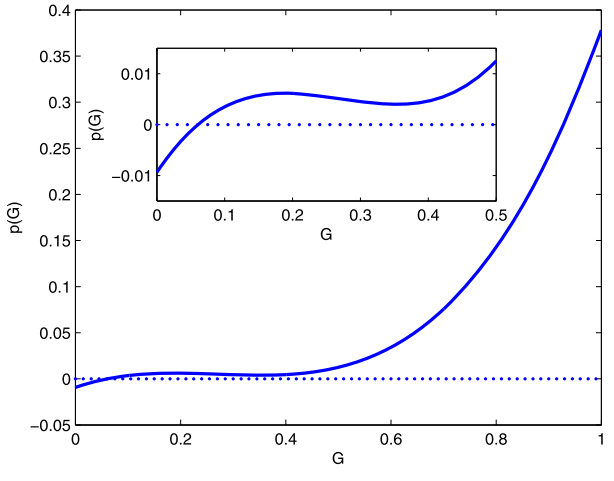

(e) $\beta = 0.8$

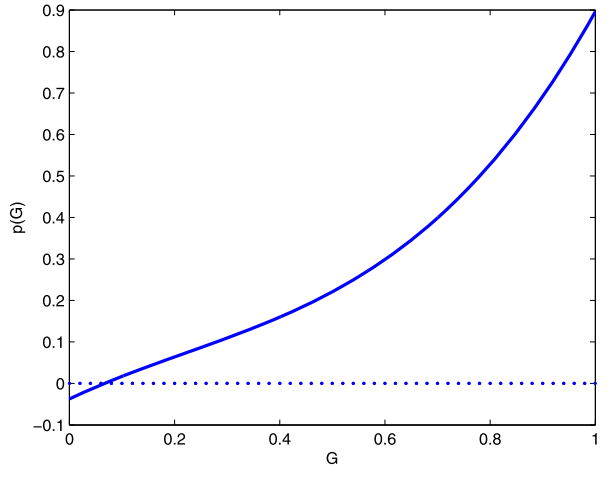

(f) $\beta = 1$

Fig. 2. Graphs of $p(G)$ with the parameters in Table 1.

(2) If $a \leq 9$, by straightforward calculation, we have

$$\begin{aligned} p(x_1) &= \frac{2}{27}p_1^3 + \frac{2}{27}p_1^2\sqrt{p_1^2 - 3p_2} - \frac{1}{3}p_1p_2 - \frac{2}{9}p_2\sqrt{p_1^2 - 3p_2} + p_3 \\ &= \frac{2}{27}(p_1 + \sqrt{p_1^2 - 3p_2})(p_1^2 - 3p_2) - \frac{1}{9}p_1h^2a_1(a_3 - 9) < 0, \end{aligned} \tag{3.16}$$

and

$$\begin{aligned} p(x_2) &= \frac{2}{27}p_1^3 - \frac{2}{27}p_1^2\sqrt{p_1^2 - 3p_2} - \frac{1}{3}p_1p_2 + \frac{2}{9}p_2\sqrt{p_1^2 - 3p_2} + p_3 \\ &< -\frac{1}{9}p_1p_2 - \frac{2}{27}(p_1^2 - 3p_2)^{3/2} + p_3 \\ &= -\frac{1}{9}p_1h^2a_1(a_3 - 9) - \frac{2}{27}(p_1^2 - 3p_2)^{3/2} < 0. \end{aligned} \tag{3.17}$$

Thus $p(x_1)p(x_2) > 0$ and $p(G)$ has exactly one positive zero (like Fig. 2 (b)).

We would also need that $G < 1$ for a coexistence equilibrium. It is easy to know that if $\beta \geq \frac{\mu\gamma(1+h^2)}{m+Mh^2} + \gamma$, then $p(1) \geq 1$; and if $\beta \geq \frac{2(\mu+m)\gamma}{3m+Mh^2}$, then $x_2 \leq 1$. By a simple calculation, we know that $\frac{\mu\gamma(1+h^2)}{m+Mh^2} + \gamma > \frac{2(\mu+m)\gamma}{3m+Mh^2}$. Set

$$H_0 = \frac{\mu\gamma(1+h^2)(m+\mu-am)}{m(m+\mu-am)+am\mu h^2} + \gamma. \tag{3.18}$$

Then when $\beta > H_0$, we have $G < 1$ if $p(G) = 0$.

Summarizing the above discussions, we obtain the following theorem.

Theorem 3.2. *Let $M, m, \mu, \gamma, \beta, h$ be positive parameters such that $\beta > \gamma$, let a be defined as in Eq. (3.13), and let H_0, H_1, H_2 be defined as in Eq. (3.18) and Eq. (3.15) respectively. Then we have*

- *If $0 < \beta \leq H_0$, system (2.4) has a unique nonnegative equilibrium $E^0 = (1, 0)$.*
- *If $\beta > H_0$, besides E^0, system (2.4) has at least one coexistence equilibrium.*
  - *(1) If $a \leq 9$, system (2.4) has a unique simple coexistence equilibrium $E_0^* = (G_0^*,\ T_0^*)$.*
  - *(2) If $a > 9$, then*
    - *(i) If $H_0 < \beta < H_1$, there is only one coexistence equilibrium $E_1^* = (G_1^*, T_1^*)$;*
    - *(ii) If $\beta = H_1$, there are two coexistence equilibria E_1^* and $E_2^* = (G_2^*, T_2^*)$, where $G_2^* < G_1^*$;*
    - *(iii) If $H_1 < \beta < H_2$, there are three coexistence equilibria E_1^*, E_2^* and $E_3^* = (G_3^*, T_3^*)$, where $G_3^* < G_2^* < G_1^*$;*
    - *(iv) If $\beta = H_2$, there are two coexistence equilibria E_2^* and E_3^*, where $G_3^* < G_2^*$;*
    - *(v) If $\beta > H_2$, there is only one coexistence equilibrium E_3^*.*

Fig. 3 shows the bifurcation diagram of positive equilibria with respect to parameter (a, β) with other parameters given by Table 1 except M which determines a. For a fixed $a > 0$, each of $\beta = H_i$ $(i = 0, 1, 2)$ is a bifurcation point of positive equilibria. For any $a > 0$, $\beta = H_0$ is a transcritical bifurcation point where a positive equilibrium bifurcates from the boundary equilibrium $E^0 = (1, 0)$. For $a > 9$, $\beta = H_1$ and $\beta = H_2$ are two saddle-node bifurcation points, with $\beta = H_1$ a forward one and $\beta = H_2$ a backward one (see Fig. 4(a)). The entire bifurcation diagram is a reversed-S shape. When $a = 9$, the two saddle-node bifurcation points merge at a codimension-two cusp bifurcation point, which is similar to the insect outbreak

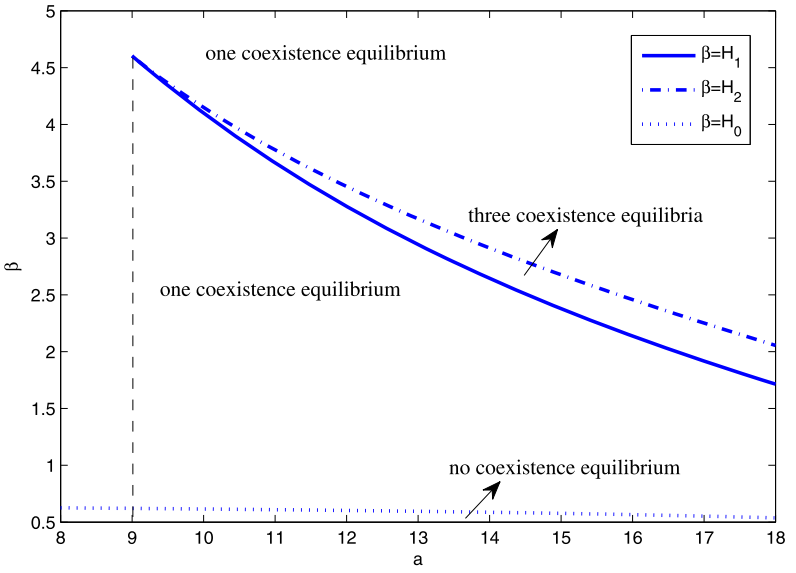

Fig. 3. The number of coexistence equilibria of system (2.4) for different values of (a, β). Here other parameters are given by Table 1 except M, which is a variable.

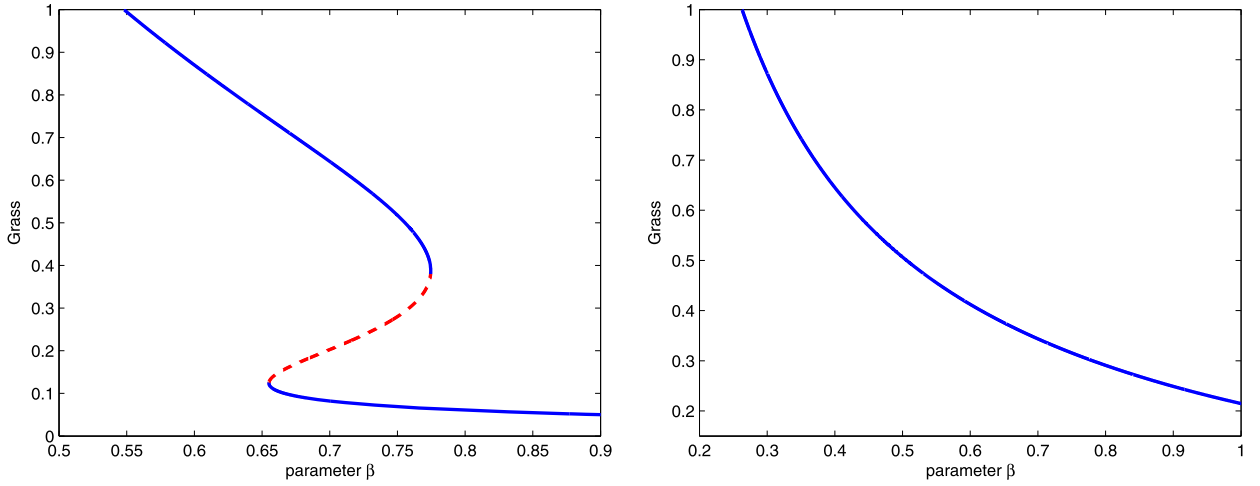

(a) $a = 17.3333 > 9$ (b) $a = 2.1333 < 9$

Fig. 4. The bifurcation diagrams of positive equilibria with respect to parameter β of system (2.4). Here the parameters in (a) are given by Table 1, and the ones in (b) are given by Table 2. In (a), $H_0 = 0.5486$, $H_1 = 0.6551$, $H_2 = 0.7746$; and in (b), $H_0 = 0.2630$.

Table 2
Parameters values for equation (2.4).

Parameter	μ	γ	h	M	m
Value	0.15	0.1	0.063	0.6	0.025

model studied in [7,18]. When $a < 9$, only the transcritical bifurcation at $\beta = H_0$ occurs, and the bifurcation diagram is a monotone one (see Fig. 4(b)).

3.3. Stability of equilibria

In this subsection, we analyze the stability of the equilibria. To determine the local stability of those equilibria, we consider the Jacobian matrix of system (2.4):

$$J = \begin{pmatrix} -\mu - \beta T & -\mu + \gamma - \beta G \\ -w(G) + w'(G)(1 - G - T) & -w(G) - \gamma \end{pmatrix}. \tag{3.19}$$

It is easy to see that the trace of J is $tr(J) = -\mu - \beta T - w(G) - \gamma < 0$ for any (G, T). Thus the local stability of equilibria is determined by the sign of the determinant $Det(J)$.

The Jacobian matrix of system (2.4) at E^0 is

$$J_{E^0} = \begin{pmatrix} -\mu & -\mu + \gamma - \beta \\ -\dfrac{Mh^2 + m}{1 + h^2} & -\dfrac{Mh^2 + m}{1 + h^2} - \gamma \end{pmatrix}. \tag{3.20}$$

Then,

$$Det(J_{E^0}) = \mu\gamma + \frac{Mh^2 + m}{1 + h^2}(\gamma - \beta) \tag{3.21}$$

Together with Theorem 3.1, we have the following result:

Theorem 3.3. *Let M, m, μ, γ, β be positive parameters such that $\beta > \gamma$, and let H_0 be defined as in Eq. (3.18). Then, we have*

(1) *If $\beta \le H_0$, E^0 is globally asymptotically stable.*
(2) *If $\beta > H_0$, E^0 is an unstable saddle.*

Next we show the stability of a coexistence equilibrium E^*. By Eq. (3.3) and Eq. (3.5), at a coexistence equilibrium, we have

$$T^*(\mu - \gamma + \beta G^*) = \mu(1 - G^*), \tag{3.22}$$

$$T^*(w(G^*) + \gamma) = w(G^*)(1 - G^*), \tag{3.23}$$

$$\mu\gamma = (\beta G^* - \gamma)w(G^*). \tag{3.24}$$

Then for the sign of $Det(J)$ at a coexistence equilibrium, we obtain

$$\begin{aligned} Det(J_{E^*}) &= \mu\gamma + \beta T(w(G^*) + \gamma) + w'(G^*)(1 - G^* - T^*)(\mu - \gamma + \beta G^*) + (\gamma - \beta G^*)w(G^*) \\ &= \beta w(G^*)(1 - G^*) + w'(G^*)(1 - G^*)(\beta G^* - \gamma) \\ &= (1 - G^*)(\beta G^* - \gamma)(w'(G^*) - f'(G^*)) \\ &= (1 - G^*)(\beta G^* - \gamma)F'(G^*). \end{aligned} \tag{3.25}$$

Therefore, when $F'(G^*) < 0$, the equilibrium is an unstable saddle, and when $F'(G^*) > 0$ the equilibrium is locally stable (stable node or stable spiral). Summarizing the above discussion, and together with Theorem 3.1 and Poincaré–Bendixon theory, we obtain the following theorem.

Theorem 3.4. *Let M, m, μ, γ, β be positive parameters such that $\beta > \gamma$ and $\beta > H_0$.*

(1) *If $a \le 9$, then E_0^* is globally asymptotically stable.*
(2) *If $a > 9$, then E_1^* and E_3^* are locally asymptotically stable, and E_2^* is an unstable saddle. Moreover, if E_1^* or E_3^* is the unique positive equilibrium, then it is also globally asymptotically stable.*

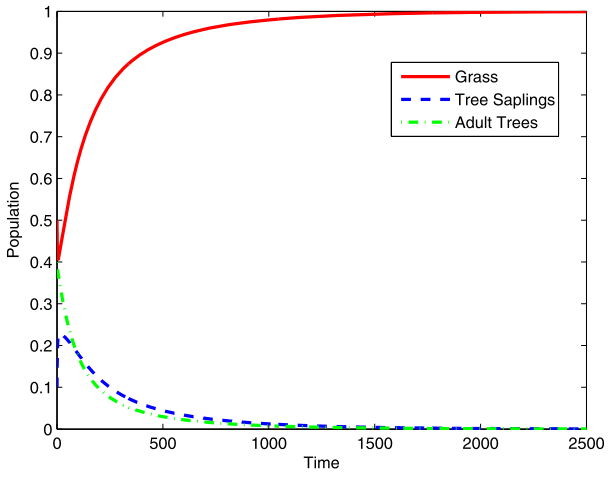

(a) $G(0) = 0.5,\ S(0) = 0.1,\ T(0) = 0.4, \beta = 0.5$

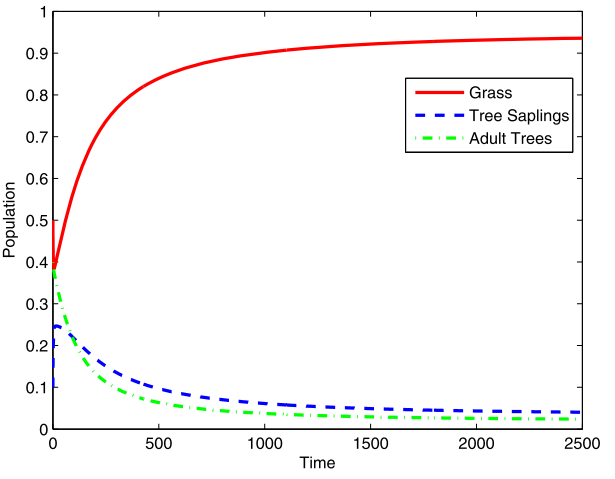

(b) $G(0) = 0.5,\ S(0) = 0.1,\ T(0) = 0.4, \beta = 0.57$

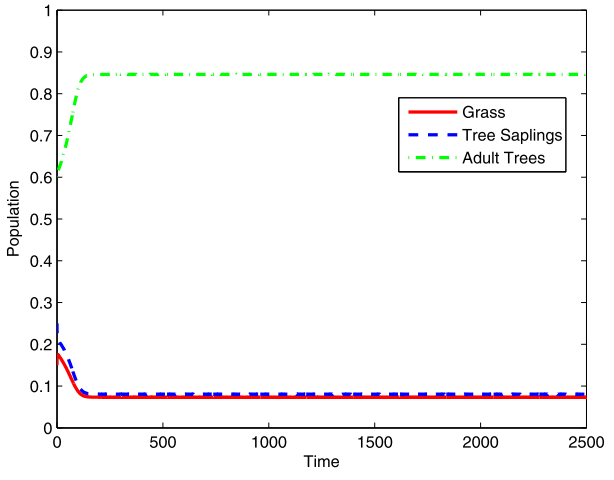

(c) $G(0) = 0.15,\ S(0) = 0.25,\ T(0) = 0.6, \beta = 0.73$

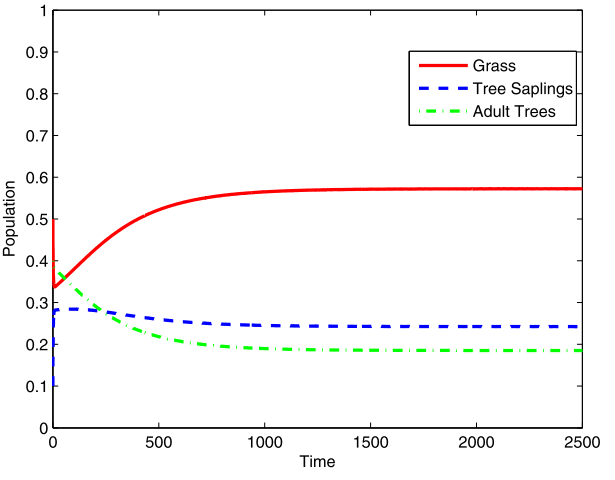

(d) $G(0) = 0.5,\ S(0) = 0.1,\ T(0) = 0.4, \beta = 0.73$

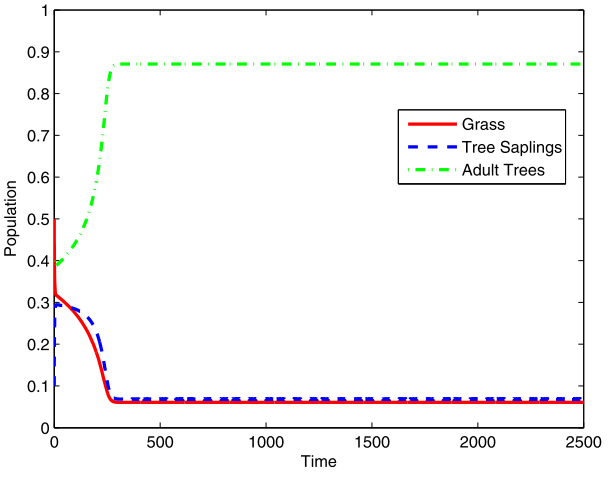

(e) $G(0) = 0.5,\ S(0) = 0.1,\ T(0) = 0.4, \beta = 0.8$

Fig. 5. Time series of system (2.1) with parameters in Table 1 and different β.

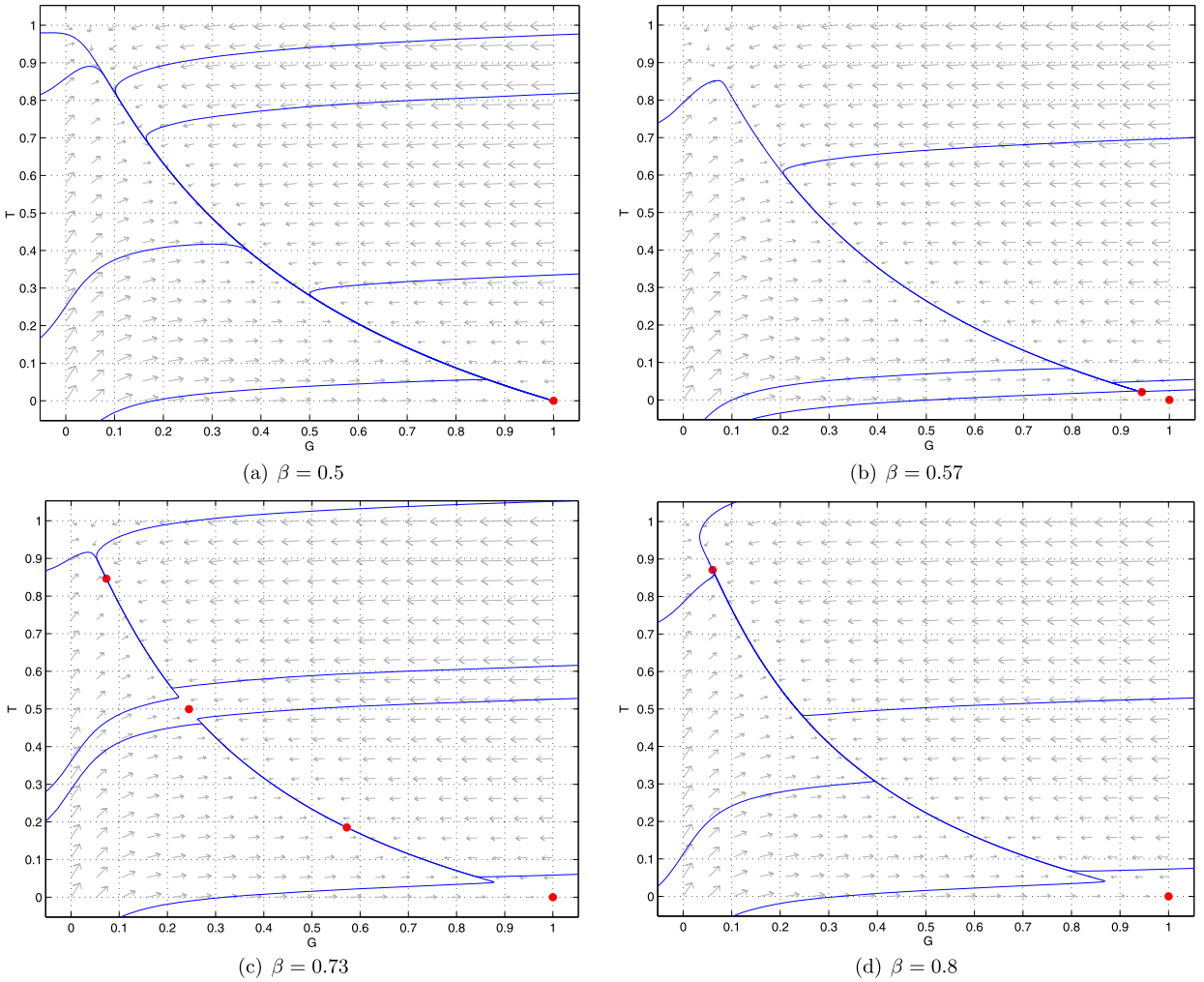

Fig. 6. Phase portraits of system (2.4) with parameters in Table 1.

Fig. 5 shows the asymptotic behavior of solutions to (2.1) for different β values, and Fig. 6 shows the corresponding phase portraits of (2.4) for the same parameters. When $\beta < H_0$, the entire landscape is occupied by the grass, and there are no trees (see Fig. 5(a) and Fig. 6(a)); and when $H_0 < \beta < H_1$, the grass and trees coexist but grass is still in dominating percentage (see Fig. 5(b) and Fig. 6(b)). Next when $H_1 < \beta < H_2$, the bistability occurs: if the initial value of trees is large, the ecosystem converges to a final state with high percentage of trees and low percentage of grass (see Fig. 5(c) and Fig. 6(c)); and if the initial value of trees is low, then the ecosystem still returns to an equilibrium of with about equal amount of grass and trees (including saplings) (see Fig. 5(d) and Fig. 6(c)). Finally when $\beta > H_2$, the trees are in commanding high percentage with only very little grass (see Fig. 5(e) and Fig. 6(d)).

4. Conclusions

In this paper, we provide a specific function form of the tree recruiting rate in the grassland-forest model (2.1) proposed in [16], and use it to qualitatively and quantitatively analyze the model (2.1) and its reduced form (2.4). We rigorously prove the existence and exact number of positive equilibria for all parameter ranges, and the stability of all the equilibria are also shown. By proving that the system does not have limit cycles, we also classify the dynamics of the system according to the number of equilibria. In particular,

the critical values at which bifurcations and stability switches occur are explicitly derived, which could be useful for practitioners to determine the ecosystem structure if system parameters can be estimated from field data.

We identify two important parameters β (sapling establishment rate) and $a = \dfrac{M(m+\mu)}{m(M+\mu)}$ which determine the regimes of "grass dominating", "tree dominating" and "alternative stable states". The parameter a is essentially the ratio of the maximum tree recruitment rate M and the minimum one m, which are in turn affected by the rainfall. Note that the key condition $a > 9$ (see Theorem 3.2) for hysteresis bifurcation diagram holds if $M/m > 9$. We believe that the numerical value 9 here is related to our choice of $n = 2$ in the Hill's function $\omega(G)$, and it would be interesting to know how that value change for larger n which makes the sigmoid recruitment function having a sharper transition at $G = h$. Other parameters also affect the bifurcation values $\beta = H_0, H_1$ and H_2, as these values are explicitly calculated in this paper. For example, H_1 and H_2 are proportional to h^{-1}, which is related to fire spreading.

Note that the model from [16] is still a minimal one, and models with more complexity have been developed in [17] and [12] in which time-periodic oscillations and spatial effect have been considered. It would be interesting to obtain more detailed results for these models using the form of tree recruiting rate provided here.

Acknowledgments

This work was done when D. D. visited Department of Mathematics, College of William and Mary during the academic year 2015–16, and she thanks Department of Mathematics, College of William and Mary for their support and kind hospitality. This work is partially supported by National Natural Science Foundation of China grant 11401140, China Scholarship Council, and US-NSF grants DMS-1313243, DMS-1331021.

References

[1] S. Archibald, D.P. Roy, V. Wilgen, W. Brian, R.J. Scholes, What limits fire? An examination of drivers of burnt area in Southern Africa, Glob. Change Biol. 15 (3) (2009) 613–630.
[2] B.E. Beisner, D.T. Haydon, K. Cuddington, Alternative stable states in ecology, Front. Ecol. Environ. 1 (7) (2003) 376–382.
[3] S.R. Carpenter, Eutrophication of aquatic ecosystems: bistability and soil phosphorus, Proc. Natl. Acad. Sci. USA 102 (29) (2005) 10002–10005.
[4] J.-F. Jiang, J.-P. Shi, Bistability dynamics in structured ecological models, in: R.S. Cantrell, C. Cosner, S.-G. Ruan (Eds.), Spatial Ecology, in: Chapman & Hall/CRC Math. Comput. Biol. Ser., Chapman & Hall/CRC, 2009, pp. 33–62.
[5] W.C. Jordan-Cooley, R.N. Lipcius, L.B. Shaw, J. Shen, J.-P. Shi, Bistability in a differential equation model of oyster reef height and sediment accumulation, J. Theoret. Biol. 289 (2011) 1–11.
[6] X. Li, H. Wang, Z. Zhang, A. Hastings, Mathematical analysis of coral reef models, J. Math. Anal. Appl. 416 (1) (2014) 352–373.
[7] D. Ludwig, D.D. Jones, C.S. Holling, Qualitative analysis of insect outbreak systems: the spruce budworm and forest, J. Anim. Ecol. 47 (1) (1978) 315–332.
[8] P.J. Mumby, A. Hastings, H.J. Edwards, Thresholds and the resilience of Caribbean coral reefs, Nature 450 (7166) (2007) 98–101.
[9] M. Scheffer, S. Carpenter, J.A. Foley, C. Folke, B. Walker, Catastrophic shifts in ecosystems, Nature 413 (6856) (2001) 591–596.
[10] M. Scheffer, S.R. Carpenter, Catastrophic regime shifts in ecosystems: linking theory to observation, Trends Ecol. Evol. 18 (12) (2003) 648–656.
[11] M. Scheffer, S.H. Hosper, M.L. Meijer, B. Moss, E. Jeppesen, Alternative equilibria in shallow lakes, Trends Ecol. Evol. 8 (8) (1993) 275–279.
[12] E. Schertzer, A.C. Staver, S.A. Levin, Implications of the spatial dynamics of fire spread for the bistability of savanna and forest, J. Math. Biol. 70 (1–2) (2015) 329–341.
[13] R.J. Scholes, Convex relationships in ecosystems containing mixtures of trees and grass, Environ. Resour. Econ. 26 (4) (2003) 559–574.
[14] H.-Y. Shu, X. Hu, L. Wang, J. Watmough, Delay induced stability switch, multitype bistability and chaos in an intraguild predation model, J. Math. Biol. 71 (6–7) (2015) 1269–1298.
[15] A.C. Staver, S. Archibald, S.A. Levin, The global extent and determinants of savanna and forest as alternative biome states, Science 334 (6053) (2011) 230–232.
[16] A.C. Staver, S. Archibald, S.A. Levin, Tree cover in sub-Saharan Africa: rainfall and fire constrain forest and savanna as alternative stable states, Ecology 92 (5) (2011) 1063–1072.

[17] A.C. Staver, S.A. Levin, Integrating theoretical climate and fire effects on savanna and forest systems, Amer. Nat. 180 (2) (2012) 211–224.
[18] S.H. Strogatz, Nonlinear Dynamics and Chaos: With Applications to Physics, Biology, Chemistry, and Engineering, 2nd edition, Westview Press, 2014.
[19] M.D. Swaine, W.D. Hawthorne, T.K. Orgle, The effects of fire exclusion on savanna vegetation at Kpong, Ghana, Biotropica 24 (2) (1992) 166–172.
[20] F. Van Langevelde, C.A.D.M. Van De Vijver, L. Kumar, J. Van De Koppel, N. De Ridder, J. Van Andel, A.K. Skidmore, J.W. Hearne, L. Stroosnijder, W.J. Bond, H.T.P. Herbert, M. Rietkerk, Effects of fire and herbivory on the stability of savanna ecosystems, Ecology 84 (2) (2003) 337–350.